

Macroscopic heterogeneity of liver fat: an MR-based study in type-2 diabetic patients

Violaine Capitan · Jean-Michel Petit · Serge Aho ·
Pierre-Henri Lefevre · Sylvain Favelier ·
Romaric Loffroy · Patrick Hillon · Denis Krausé ·
Jean-Pierre Cercueil · Boris Guiu

Received: 20 December 2011 / Revised: 5 March 2012 / Accepted: 17 March 2012 / Published online: 5 May 2012
© European Society of Radiology 2012

Abstract

Objective To assess the heterogeneity of liver fat deposition with MR of the liver in type-2 diabetic (T2D) patients.

Methods We enrolled 121 consecutive T2D patients. The reference standard was 3.0-T ¹H-MR spectroscopy. Hepatic steatosis was defined as liver fat content (LFC) ≥ 5.56 %. A triple-echo gradient-echo sequence corrected for T1 recovery and T2* decay was used to calculate LFC in left and right

livers and hepatic segments. Analyses were performed using a linear mixed model.

Results Fifty-nine (48.8 %) patients had liver steatosis, whereas 62 (51.2 %) did not. Steatosis was greater in the right than in the left liver ($P < 0.0001$) [mean difference: 1.32 % (range: 0.01–8.75 %)]. In seven patients (5.8 %), LFC was < 5.56 % in one side of the liver, whereas it was ≥ 5.56 % in the other.

Steatosis of the left and right liver was heterogeneous at the segmental level in both non-steatotic ($P < 0.001$ and $P < 0.0001$ respectively) and steatotic ($P < 0.0001$ and $P = 0.0002$ respectively) patients [mean maximum difference: 3.98 % (range: 0.74–19.32 %)]. In 23 patients (19 %), LFC was < 5.56 % in one segment, whereas it was ≥ 5.56 % in at least one other.

Conclusion Overall, the mean segmental/lobar variability of steatosis is low. However, segmental variability can sometimes lead to a misdiagnosis.

Key Points

- There is a need for methods quantifying steatosis over a large region.
- Steatosis is usually greater in the right than left lobe of the liver.
- Steatosis within both left and right hepatic lobes is segmentally heterogeneous.
- Segmental variability of steatosis can result in misdiagnosis.

Keywords MR spectroscopy · Liver fat content · Type-2 diabetes · Gradient-echo sequence · Variability

Introduction

Nonalcoholic fatty liver disease (NAFLD) is now the most common form of chronic liver disease in adults in Western countries [1]. It encompasses a broad spectrum of liver abnormalities ranging from steatosis to steatohepatitis, cirrhosis and

V. Capitan (✉) · P.-H. Lefevre · S. Favelier · R. Loffroy ·
D. Krausé · J.-P. Cercueil · B. Guiu (✉)
Department of Radiology, CHU (University Hospital),
14 rue Paul Gaffarel, BP 77908, 21079 Dijon, France
e-mail: violaine19.capitan@laposte.net

B. Guiu
e-mail: boris.guiu@chu-dijon.fr

J.-M. Petit
Department of Endocrinology, Diabetology,
and Metabolic Diseases, CHU (University Hospital),
BP 77908, 21079 Dijon, France

S. Aho
Department of Biostatistics and Medical Informatics,
CHU (University Hospital), BP 77908,
21079 Dijon, France

P. Hillon · J.-P. Cercueil · B. Guiu
University of Burgundy, INSERM U866, BP 87900,
21079 Dijon, France

P. Hillon
Department of Hepatology, CHU (University Hospital),
BP 77908, 21079 Dijon, France

V. Capitan · J.-M. Petit · S. Aho · P.-H. Lefevre · S. Favelier ·
R. Loffroy · P. Hillon · D. Krausé · J.-P. Cercueil · B. Guiu
CHU (University Hospital), BP 77908,
21079 Dijon, France

hepatocellular carcinoma. Though laboratory test abnormalities and radiological findings may suggest NAFLD, histological evaluation by liver biopsy is still considered the reference standard for diagnosing NAFLD and quantifying liver fat [2]. At histology, NAFLD lesions are unevenly distributed throughout the liver, leading to a potential sampling bias when biopsy is used to assess steatosis [2–4]. Moreover, liver biopsy is invasive, which strongly limits its use in clinical practice given the high prevalence of NAFLD. Therefore, many noninvasive methods, especially radiological, have been developed over time. Among them, proton magnetic resonance spectroscopy ($^1\text{H-MRS}$) is now regarded as the most accurate noninvasive technique for the quantification of steatosis [5–7], and thus is extensively used in published series. $^1\text{H-MRS}$ is able to quantify the proportion of fatty protons within a far larger volume than that from biopsy specimens. Although sampling bias due to the microscopic variability of steatosis is strongly limited, $^1\text{H-MRS}$ is usually performed in only one hepatic segment and supposes that steatosis is homogeneous at the macroscopic level. However, many studies have reported focal fatty sparing or infiltration at liver imaging [8]. In such cases, $^1\text{H-MRS}$ could potentially underestimate or overestimate the liver fat fraction, according to the region of interest (ROI) studied. The frequency of such focal fatty sparing or infiltration as well as the degree of heterogeneity in fat deposition within the liver remains unknown.

Other MR-imaging methods based on differences in the resonance frequencies of fat and water protons (also called chemical-shift gradient-echo imaging) have been developed [7, 9, 10]. Interestingly, these techniques have the potential to assess steatosis in the entire liver parenchyma. Recently, the triple-echo technique has demonstrated an excellent correlation and concordance with regard to $^1\text{H-MRS}$ [7], and is able to provide reliable liver fat maps for the estimation of steatosis [11]. Type-2 diabetes is closely linked to NAFLD and provides a model of choice for the study of liver steatosis, given its high prevalence [12] and the wide variations in liver fat content (LFC) in this condition [7].

Thus, the aim of this study was to assess the macroscopic heterogeneity of liver fat deposition in type-2 diabetic patients using the triple-echo MR technique.

Materials and methods

This prospective, single-centre study was approved by our regional ethics committee. Written informed consent was obtained from all patients before study inclusion.

Patients

Between October 2009 and September 2011, consecutive patients were screened at the endocrinology department of

our institution for the following inclusion criteria: type-2 diabetes; age older than 18 years; body weight less than 150 kg (the MRI table weight limit); no known acute or chronic diseases based on the patient's medical history, physical examination and standard laboratory tests; alcohol consumption <20 g/day; no evidence of liver disease such as viral hepatitis. Patients were hospitalised in order to initiate insulin therapy (in patients with diabetes not controlled with an oral hypoglycaemic agent), or for annual disease assessment or for educative interventions in outpatient hospitalisation.

Patients with claustrophobia or with a pacemaker or metallic implant contraindicating the MR study ($n=3$) were excluded. Therefore, this study was conducted in 121 patients with a mean age of 53 years (range, 37–81 years). There were 54 women and 67 men.

MR imaging

MR imaging was performed using 3.0 T (Magnetom Trio Tim; Siemens, Erlangen, Germany) with a peak gradient amplitude of 45 mT/m and a time-to-peak of 204 μs . A six-element body phased-array coil system was used.

All patients were carefully instructed to suspend respiration in expiration and to be consistent in their breath holds. To allow correct positioning, localising sequences in the coronal, transverse and sagittal planes were acquired during a breath-hold. A transverse breath-hold low T1-weighted two-dimensional triple-echo spoiled gradient-echo sequence was performed with the following parameters: repetition time (ms)/echo time (ms) of 192/2.46 [in-phase (IP_1)], 3.69 [opposed-phase (OP)] and 4.92 [in-phase (IP_2)]; flip angle, 20°; section thickness, 6 mm; intersection gap, 1.2 mm; matrix, 256*192; number of sections, 25; and acquisition time, 34 s. Parallel imaging (with an acceleration factor of 2) was performed using generalised autocalibrating partially parallel acquisition (GRAPPA; Siemens Medical Solutions Erlangen, Germany). Two separate breath holds (each lasting 17 s) were needed to cover the entire liver volume.

$^1\text{H-MR}$ spectroscopy

Semi-automated optimisation of gradient shimming followed by manual adjustment of central frequency was performed, and water line widths of less than 25 Hz were obtained. Water suppression was not performed for any of the sequences.

Single-voxel MR spectroscopic data were acquired using seven breath-hold point-resolved spatially localised spectroscopic pulse sequences (repetition time, 5,000 ms; 3 acquisitions; 2,048 data points over 1,250-Hz spectral width; and acquisition time, 15 s) with echo times of 30, 40, 50, 60, 80, 100 and 135 ms to measure the T2 relaxation times of water and CH_2 .

In all patients, the same 30*30*30-mm (27 ml) voxel was used for these seven sequences and was positioned obliquely on segment VII on the transverse low T1-weighted section (avoiding extra-hepatic fat, large hepatic vessels and organs adjacent to the liver).

¹H-MR spectroscopic data analysis

¹H-MR spectroscopic data were interpreted by a radiologist who was blinded to the MR imaging results. The Java-based MR user interface spectroscopic analysis package (jMRUI; A. van den Boogaart, Catholic University, Leuven, Belgium) [13] was used for time-domain analysis. Metabolite signals were analysed using the advanced magnetic resonance fitting algorithm within jMRUI. We measured the water peak at 4.76 ppm and the methylene peak at 1.33 ppm. Spectra were used only if homogeneity after shimming, measured as the full width at 50 % peak height, was better than 0.40 ppm. Peak integrals were quantified by fitting to a Gaussian line shape.

T2 relaxation times of both metabolites were determined from their peak amplitudes at each echo time using an exponential least-squares fitting algorithm. The peak areas of the methylene and water signals were then corrected for T2 effects (i.e., theoretical peak areas with 0 echo time), using the means of previously calculated T2 relaxation times, as previously reported [7].

LFC was calculated as follows:

$$\text{LFC}_{\text{MRS}} = 100 * A_{0\text{ms_CH}_2} / (A_{0\text{ms_CH}_2} + A_{0\text{ms_WATER}})$$

where $A_{0\text{ms_CH}_2}$ and $A_{0\text{ms_WATER}}$ were the areas of the methylene and water peaks, respectively, corrected for both T1 and T2 effects. Hepatic steatosis was defined as $\text{LFC} \geq 5.56\%$ [14, 15].

Quantification of LFC in each region of interest

MR imaging results were interpreted by consensus by two radiologists, who were blinded to the ¹H-MRS findings. On the low T1-weighted triple-echo gradient-echo sequence and for each patient, we drew a 2D region of interest (ROI) measuring 2–3 cm in diameter in each hepatic segment on three successive slices (Fig 1). Signal intensity in each ROI was recorded for IP₁ (TE=2.46 ms), OP (TE=3.69 ms) and IP₂ (TE=4.92 ms) of the triple-echo sequence. We used the “copy and paste” function of the workstation (Leonardo; Siemens, Erlangen, Germany) to draw exactly the same ROIs at the same locations on the IP and OP images. The signal intensity for each segment was obtained by averaging the signal intensity in the corresponding ROIs of the three successive slices. The signal intensity recorded for the left liver was obtained by averaging the signal intensity of the ROIs drawn in segments II, III and IV, whereas the signal intensity

for the right liver was obtained by averaging the signal intensity of the ROIs in segments V, VI, VII and VIII. Fat fraction values were calculated as previously reported [7].

The IP signal intensity corrected for T2* decay ($\text{SI}_{\text{IP_corrected}}$) was computed as $\text{SI}_{\text{IP}} \cdot e^{(-\Delta\text{TE}/T2^*)}$ [16], where SI_{IP} was the IP₁ signal intensity and ΔTE was the echo time difference between IP and OP states (i.e., $\Delta\text{TE}=1.23$ ms at 3.0 T). Thus, LFC within each ROI was computed as follows:

$$\text{LFC} = 100 * (\text{SI}_{\text{IP_corrected}} - \text{SI}_{\text{OP}}) / (2 * \text{SI}_{\text{IP_corrected}})$$

where SI_{OP} was OP signal intensity. The problem of fat-water ambiguity due to chemical-shift gradient-echo imaging is not relevant when assessing liver steatosis, since many ¹H-MRS studies [1, 7, 11, 17] support the hypothesis that steatosis exceptionally exceeds 50 %. A total of 968 fat fractions were recorded in the 121 patients of our study. To visually check the validity of the fat fractions in each ROI, a fat map was built from basic image calculation functions of the workstation [11].

Statistical analysis

The relationship between LFC measured by ¹H-MRS and the triple-echo technique was estimated using simple linear regression. Pearson’s correlation coefficient was calculated. A robust variance estimator was used to take into account the non-Gaussian distributions of the two variables and heteroscedasticity (i.e., unequal variances). We computed Lin’s concordance coefficient ρ_c [18], which combines measurements of precision and accuracy to determine whether the observed data deviate significantly from the line of perfect agreement (i.e. the 45° line).

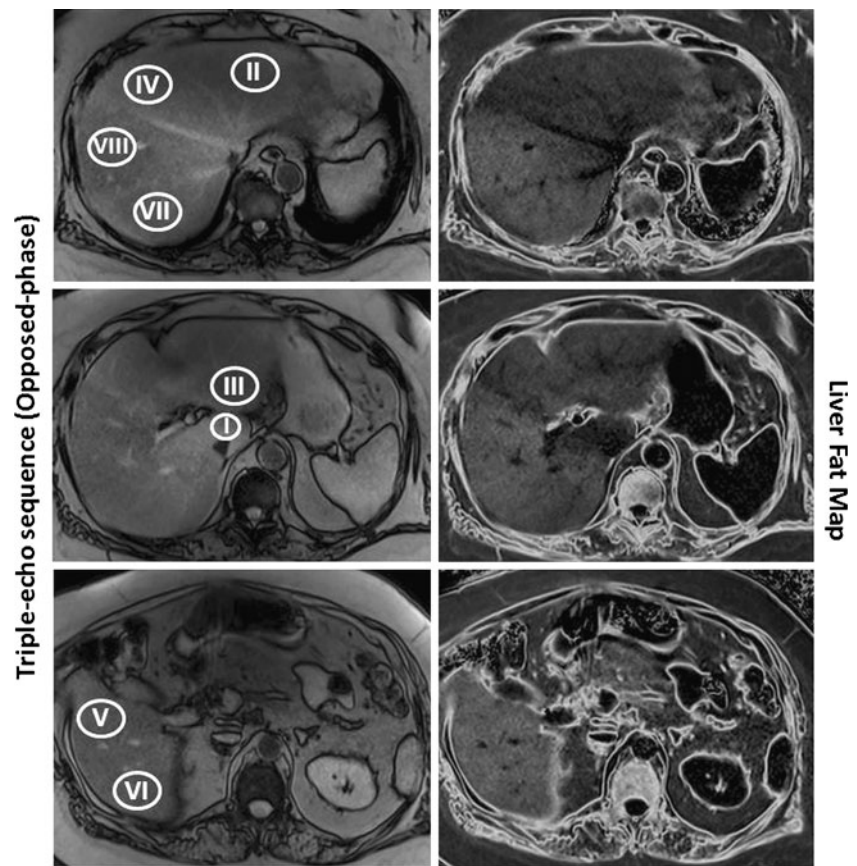
Heterogeneity of liver steatosis was assessed using a linear mixed model in order to take into account the spatial correlation of the data estimated using the intraclass correlation coefficient. Multiple comparison adjustments were performed using the following tests: Sidak, Scheffé and Tukey-Kramer. The normality of residuals and their homoscedasticity (i.e. underlying assumptions with linear models) were verified. All statistical analyses were performed using STATA software version 11.0 (Statacorp, College Station, TX). P values < 0.05 were considered significant.

Results

We confirm here that the ¹H-MRS and triple-echo techniques have excellent agreement: Pearson’s correlation coefficient and Lin’s concordance coefficient were 0.973 ($P < 0.0001$) and 0.969 ($P < 0.0001$), respectively.

In the 121 patients, mean LFC (¹H-MRS) was 9.07 % (SD: 8.87; range: 0.48–35.56). Fifty-nine (48.8 %) had liver steatosis, whereas 62 (51.2 %) did not.

Fig. 1 Position of regions of interest in each hepatic segment on triple-echo gradient-echo sequence (on the right). Corresponding fat maps are shown on the left. Please note the lobar heterogeneity of liver steatosis (upper left) and the lower fat content in segment I (middle left)



Left vs. right liver analysis

Globally, the right liver had a greater degree of steatosis than the left ($P < 0.0001$) (Table 1). In both steatotic and non-steatotic livers, the difference was also significant ($P < 0.0001$).

In the whole population, the mean difference in LFC between the left and right liver was 1.32 % (range: 0.01–8.75 %) (Fig. 2). This difference was greater than 5.56 % in two patients (1.7 %). In seven patients (5.8 %), the LFC was < 5.56 % in one side of the liver, whereas it was ≥ 5.56 % in the other, which could account for a misdiagnosis of liver

steatosis in cases when LFC is determined in the left or right liver only.

Analysis of liver segments

LFCs calculated in all hepatic segments (Fig. 3) are summarised in Table 2 for patients with and without steatosis.

Steatosis of the left and right liver was not homogeneous at the segmental level. In patients without liver steatosis, LFC in

Table 1 Liver fat content in left and right liver

	Liver fat content (mean \pm SD)	Min–max	<i>P</i> value
All patients (n=121)			< 0.0001
Right liver	8.86 % \pm 8.55	0.78–35.62	
Left liver	7.72 % \pm 8.12	0.21–37.74	
No steatosis (n=62)			< 0.0001
Right liver	2.26 % \pm 1.38	0.78–5.75	
Left liver	1.82 % \pm 1.27	0.21–6.09	
Steatosis (n=59)			< 0.0001
Right liver	15.8 % \pm 7.32	6.38–35.62	
Left liver	13.92 % \pm 7.65	4.44–37.74	

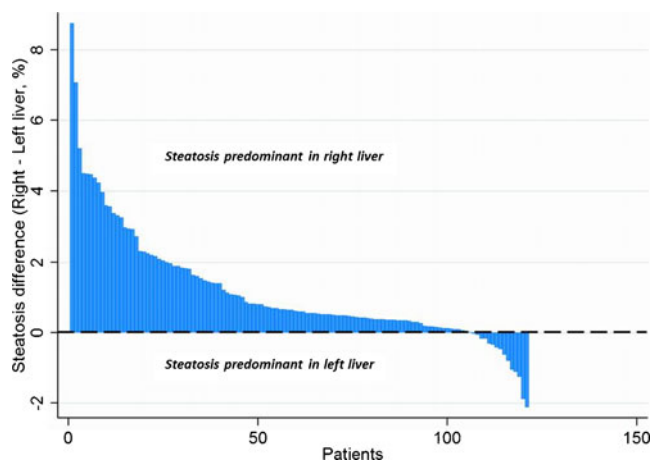


Fig. 2 Waterfall plot highlighting the differences in steatosis between the right and left liver

the left and right liver was heterogeneous ($P < 0.001$ and $P < 0.0001$, respectively). In patients with liver steatosis, LFC in the left and right liver was also heterogeneous ($P < 0.0001$ and $P = 0.0002$, respectively).

In the whole population, the average maximum difference in LFC between segments was 3.98 % (range: 0.74–19.32 %) (Fig. 4). This maximum difference between segments was greater than 5.56 % in 30 patients (24.8 %), while it was greater than 10 % in 5 patients (4.1 %). In 23 patients (19 %), LFC was < 5.56 % in one segment, whereas it was ≥ 5.56 % in at least one other segment, which could account for a misdiagnosis of liver steatosis in cases when LFC is determined in one segment only.

Discussion

Liver biopsy is the only reference standard for the assessment of liver inflammation and fibrosis, but biopsy is invasive, potentially harmful and thus not appropriate as a screening tool for NAFLD, which is highly prevalent in the population. However, liver biopsy is still considered the reference standard for diagnosing NAFLD and quantifying liver fat [2], although it may also suffer from sampling variability [4, 19]. Indeed, a liver biopsy represents only 1/50,000–1/65,000 of the whole liver [20]. The extent of steatosis is commonly assessed semi-quantitatively by reporting the percentage of hepatocytes containing fat droplets [2]. On a typical slide, fatty hepatocytes are not homogeneously distributed and exhibit a zonal distribution pattern [3], thereby suggesting substantial heterogeneity of steatosis at a microscopic level. In a pathological study reporting liver biopsies performed via an intercostal route through a single access puncture [4], the steatosis grade differed in 22 % of paired biopsy samples.

Fig. 3 Box plots of liver steatosis according to each hepatic segment (Couinaud classification). The top and bottom of the boxes are the first and third quartiles, respectively. The length of the box thus represents the interquartile range within which 50 % of the values were located. The line through the middle of each box represents the median. The error bars show the minimum and maximum values (range). An outside value (circles) is defined as a value that is smaller than the lower quartile minus 1.5 times the interquartile range, or larger than the upper quartile plus 1.5 times the interquartile range

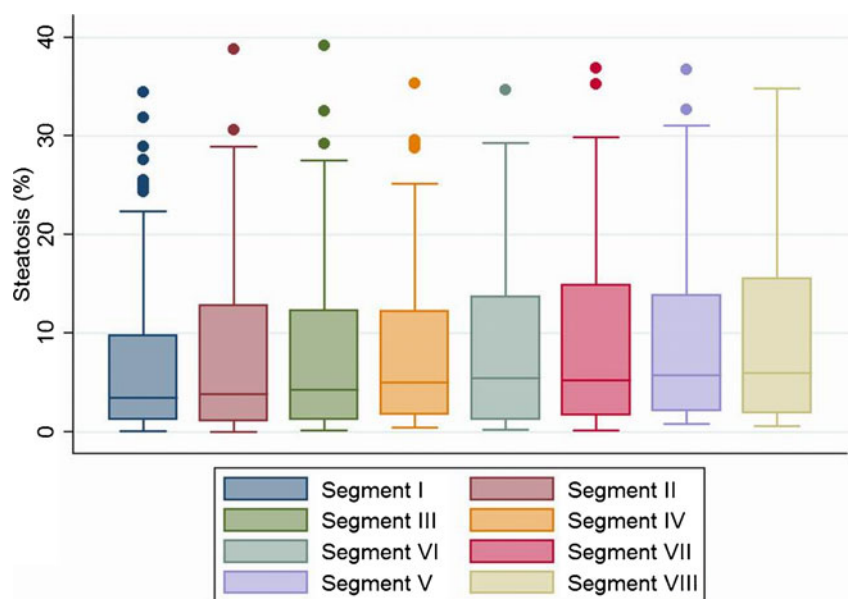


Table 2 Liver fat content in all hepatic segments (Couinaud classification)

	Liver fat content (mean ± SD)	Min–max
No steatosis (n=62)		
Segment I	1.55 %±1.13	0.05–5.67
Segment II	1.49 %±1.21	0–5.51
Segment III	1.8 %±1.6	0.11–7.5
Segment IV	2.18 %±1.31	0.41–6.28
Segment V	2.63 %±1.38	0.8–6.09
Segment VI	1.9 %±1.53	0.18–6.5
Segment VII	2.07 %±1.43	0.11–5.58
Segment VIII	2.44 %±1.52	0.6–6.23
Steatosis (n=59)		
Segment I	13.08 %±8.08	2.79–34.45
Segment II	13.27 %±7.72	3.54–38.76
Segment III	13.96 %±7.92	3.54–39.16
Segment IV	14.52 %±7.58	4.14–35.32
Segment V	15.64 %±7.29	6.27–36.75
Segment VI	15.09 %±7.11	3.54–34.63
Segment VII	15.93 %±7.9	5.06–36.85
Segment VIII	16.52 %±7.6	6.14–34.82

Two patients in this series had a sampling variability equal to or higher than 30 % in the amount of steatosis. More importantly, the intraobserver kappa reliability test was reported at only 0.74. In a very recent study reporting the concordance among four expert pathologists from different centres regarding the quantitative evaluation of liver steatosis (interobserver variability) [21], poor agreement (intraclass correlation coefficient: 0.57) was found regarding the assessment of total steatosis. This clinically unacceptable interobserver variability can be prevented by using software that objectively quantifies

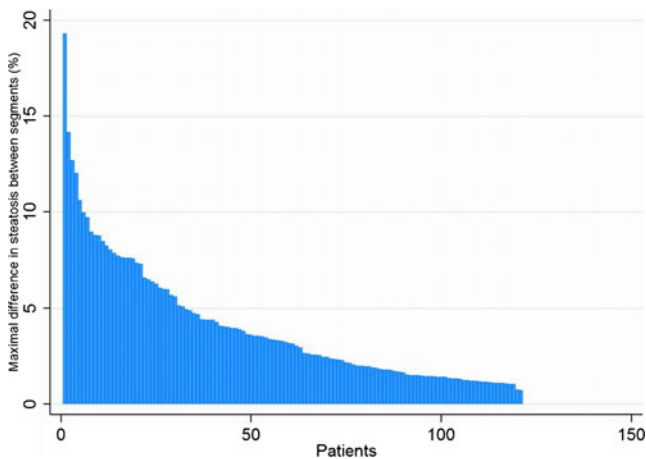


Fig. 4 Waterfall plot highlighting the maximal differences in steatosis between liver segments

the area occupied by fatty droplets in a liver section rather than the percentage of hepatocytes containing lipid droplets [21–23]. Intrahepatic lipid assay (lipid extraction and measurement) is probably the best reference for the quantification of liver fat from a biopsy sample [24], since it gives a quantitative value of intrahepatic lipid content that is not subject to interobserver variability. However, these quantitative methods are prone to sampling bias since they derive from biopsy samples whose number and size are limited. Therefore, other methods and especially radiological methods have been developed over time. Among them, $^1\text{H-MRS}$ is considered the most accurate non-invasive technique for the quantification of steatosis [5–7]. $^1\text{H-MRS}$ provides a reliable estimation of hepatic triglyceride content and allows a far larger sampling of the liver than does liver biopsy (8–27 g in a typical voxel of spectroscopy versus 50–100 mg in a biopsy sample). $^1\text{H-MRS}$ is thus less prone to sampling variability. However, as noted by Brunt et al. [25], there is parenchymal (regional or zonal) variability of lipid, glucose and insulin metabolism. Therefore, in NAFLD the disease process may not be the same throughout the liver parenchyma [25]. Two-dimensional chemical-shift imaging (CSI) could theoretically be an attractive option to assess the variation of liver fat content within the liver [17], but (1) it is very challenging to obtain an excellent shimming over a large volume of interest and (2) the long acquisition time leads to motion artefacts and prevents multiple acquisitions at different echo times essential for T2 correction, as demonstrated elsewhere [7]. Therefore, $^1\text{H-MRS}$ is typically performed in one segment (most commonly segment VII or VIII), but it is far from certain that one segment is representative of the whole liver regarding the amount of steatosis. Since the triple-echo technique, corrected for T1 bias and T2* decay, has demonstrated excellent agreement with $^1\text{H-MRS}$ and has the ability to quantify liver steatosis in each ROI of the liver [7, 11, 26], the triple-echo technique can assess the heterogeneity of steatosis at a macroscopic level.

In our study, we demonstrated a significantly higher amount of steatosis in the right than in the left liver. To our knowledge, this has never been reported in the literature. In 41 paired biopsy samples obtained from intraoperative biopsies, the pathological grading of steatosis in the left and right lobes was different in seven (17 %) [3], but no information was provided regarding the most steatotic lobe. Though we report a relatively low difference (mean: 1.32 %) in LFC in the left and right liver at the population level, at the patient level a misdiagnosis of steatosis can be observed in 5.8 % of cases, which is not negligible. The left and right livers are functionally separate with no portal or biliary drainage anastomoses [27]. Portal blood flow conveyed via the superior mesenteric vein contains dietary fat, which may result in fatty changes in hepatocytes [8]. Based on angiography and scintigraphy findings, the streamline flow theory explains why the blood from the superior mesenteric vein flows mainly into the right liver, while blood from the splenic vein flows mainly into the left liver [27, 28]. Therefore, the different portal pattern between the left and right liver might explain the difference in steatosis at a hemi-liver level.

At the segmental level, steatosis is heterogeneous in both the left and right liver as well. A mean maximum difference between segments of 3.98 % was reported over a wide range (0.74–19.32 %). This value cannot be ignored since it is close to the 5.56 % cutoff used for the diagnosis of steatosis. In most papers, monovoxel $^1\text{H-MRS}$ is used to determine LFC in one segment, based on the argument that it is not subject to the sampling bias of liver biopsy [7, 14]. In our series, the segmental heterogeneity of steatosis may account for a misdiagnosis of steatosis in 19 % of patients. Therefore, all imaging techniques measuring steatosis in only one segment are also prone to sampling error given the segmental variability of steatosis. Interestingly, segment I has the lowest LFC among all the liver segments. Some non-tumorous defects of portal perfusion described in segment I have been reported to be caused by nonportal venous return from gastric arterial arteries [29], namely the parabiliary venous system. The parabiliary venous system originates from the pancreatico-duodenal and pyloro-duodenal veins, runs along the common bile duct and divides in the liver hilum [30]. Couinaud reported that the parabiliary system supplied segment I in 44.6 % of cases [30]. Decreased portal inflow due to non-portal blood supply via the parabiliary venous system might explain why there is less fat in segment I.

Several limitations of our study must be acknowledged. Firstly, for each hepatic segment, LFC was determined from three 2D ROIs derived from three successive slices. We did not use 3D ROIs because 3D tools for signal measurement as well as the ‘copy and paste’ function were not available in our workstations. With 2D-ROIs, we did not include large

vessels or bile ducts, which could have influenced the results. In each hepatic segment, the sampled volume was smaller than the whole volume of the segment, but was in the range 5.65–12.72 cm³, which is in keeping with the volume of a typical ¹H-MRS voxel. Secondly, we used the 5.56 % cutoff [14] for steatosis determined on “normal” multiethnic individuals from Dallas in the absence of another validated cutoff in Europe. As already reported, it is unclear whether this cutoff should be generalised to European adults [31]. Thirdly, B1 field heterogeneity was not taken into account, but as we used a low flip angle with the triple-echo sequence, the B1-heterogeneity artefacts were limited. Moreover, it can be assumed that B1 inhomogeneity was similar for the three echo times we used in this sequence, thereby explaining why B1 heterogeneity artefacts were not visible on the fat maps used for visual checking. Fourthly, our results apply only to our study population, i.e. type-2 diabetic patients. Although type-2 diabetes is often linked to NAFLD, our results require further confirmation to be applied in a more general population.

In conclusion, the deposition of liver steatosis within the liver exhibits substantial heterogeneity at a macroscopic scale. This heterogeneity is segmental, even lobar. At the population level, the mean segmental or lobar variability of hepatic steatosis is relatively low. However, at the patient level, segmental variability can result in a misdiagnosis of steatosis or a substantial under- or overestimation of LFC if the method used for quantification is performed in only one segment. This potential pitfall underlines the need for methods that allow the quantification of steatosis over a large region.

Acknowledgements We would like to thank Philip Bastable for revision of the English language.

References

- Browning JD, Szczepaniak LS, Dobbins R et al (2004) Prevalence of hepatic steatosis in an urban population in the United States: impact of ethnicity. *Hepatology* 40:1387–1395
- Kleiner DE, Brunt EM, Van Natta M et al (2005) Design and validation of a histological scoring system for nonalcoholic fatty liver disease. *Hepatology* 41:1313–1321
- Merriman RB, Ferrell LD, Patti MG et al (2006) Correlation of paired liver biopsies in morbidly obese patients with suspected nonalcoholic fatty liver disease. *Hepatology* 44:874–880
- Ratziu V, Charlotte F, Heurtier A et al (2005) Sampling variability of liver biopsy in nonalcoholic fatty liver disease. *Gastroenterology* 128:1898–1906
- Johnson NA, Walton DW, Sachinwalla T et al (2008) Noninvasive assessment of hepatic lipid composition: Advancing understanding and management of fatty liver disorders. *Hepatology* 47:1513–1523
- van Werven JR, Marsman HA, Nederveen AJ et al (2010) Assessment of hepatic steatosis in patients undergoing liver resection: comparison of US, CT, T1-weighted dual-echo MR imaging, and point-resolved ¹H MR spectroscopy. *Radiology* 256:159–168
- Guiu B, Petit JM, Loffroy R et al (2009) Quantification of liver fat content: comparison of triple-echo chemical shift gradient-echo imaging and in vivo proton MR spectroscopy. *Radiology* 250:95–102
- Yoshimitsu K, Honda H, Kuroiwa T et al (2001) Unusual hemodynamics and pseudolesions of the noncirrhotic liver at CT. *Radiographics* 21:S81–S96
- Pineda N, Sharma P, Xu Q, Hu X, Vos M, Martin DR (2009) Measurement of hepatic lipid: high-speed T2-corrected multiecho acquisition at ¹H MR spectroscopy—a rapid and accurate technique. *Radiology* 252:568–576
- Yokoo T, Bydder M, Hamilton G et al (2009) Nonalcoholic fatty liver disease: diagnostic and fat-grading accuracy of low-flip-angle multiecho gradient-recalled-echo MR imaging at 1.5 T. *Radiology* 251:67–76
- Guiu B, Loffroy R, Petit JM et al (2009) Mapping of liver fat with triple-echo gradient echo imaging: validation against 3.0-T proton MR spectroscopy. *Eur Radiol* 19:1786–1793
- Targher G, Bertolini L, Rodella S et al (2007) Nonalcoholic fatty liver disease is independently associated with an increased incidence of cardiovascular events in type 2 diabetic patients. *Diabetes Care* 30:2119–2121
- Naressi A, Couturier C, Devos JM et al (2001) Java-based graphical user interface for the MRUI quantitation package. *MAGMA* 12:141–152
- Szczepaniak LS, Nurenberg P, Leonard D et al (2005) Magnetic resonance spectroscopy to measure hepatic triglyceride content: prevalence of hepatic steatosis in the general population. *Am J Physiol Endocrinol Metab* 288:E462–E468
- Kotronen A, Peltonen M, Hakkarainen A et al (2009) Prediction of non-alcoholic fatty liver disease and liver fat using metabolic and genetic factors. *Gastroenterology* 137:865–872
- Hussain HK, Chenevert TL, Londy FJ et al (2005) Hepatic fat fraction: MR imaging for quantitative measurement and display—early experience. *Radiology* 237:1048–1055
- Irwan R, Edens MA, Sijens PE (2008) Assessment of the variations in fat content in normal liver using a fast MR imaging method in comparison with results obtained by spectroscopic imaging. *Eur Radiol* 18:806–813
- Lin LI (1989) A concordance correlation coefficient to evaluate reproducibility. *Biometrics* 45:255–268
- Wieckowska A, McCullough AJ, Feldstein AE (2007) Noninvasive diagnosis and monitoring of nonalcoholic steatohepatitis: present and future. *Hepatology* 46:582–589
- Brunt EM, Tiniakos DG (2010) Histopathology of nonalcoholic fatty liver disease. *World J Gastroenterol* 16:5286–5296
- El-Badry AM, Breitenstein S, Jochum W et al (2009) Assessment of hepatic steatosis by expert pathologists: the end of a gold standard. *Ann Surg* 250:691–697
- Fiorini RN, Kirtz J, Periyasamy B et al (2004) Development of an unbiased method for the estimation of liver steatosis. *Clin Transplant* 18:700–706
- Marsman H, Matsushita T, Dierkhising R et al (2004) Assessment of donor liver steatosis: pathologist or automated software? *Hum Pathol* 35:430–435
- Raptis DA, Fischer MA, Graf R et al (2011) MRI: the new reference standard in quantifying hepatic steatosis? *Gut* 61:117–127, Epub 2011 Oct 13
- Brunt EM (2008) Do you see what I see? The role of quality histopathology in scientific study. *Hepatology* 47:771–774
- Guiu B, Petit JM, Loffroy R et al (2011) Liver methylene fraction by dual- and triple-echo gradient-echo imaging at 3.0 T:

- Correlation with proton MR spectroscopy and estimation of robustness after SPIO administration. *J Magn Reson Imaging* 33:119–127
27. Barbaro B, Palazzoni G, Prudenzano R, Cina A, Manfredi R, Marano P (1999) Doppler sonographic assessment of functional response of the right and left portal venous branches to a meal. *J Clin Ultrasound* 27:75–80
 28. Gates GF, Dore EK (1973) Streamline flow in the human portal vein. *J Nucl Med* 14:79–83
 29. Yamagami T, Arai Y, Matsueda K, Inaba Y, Sueyoshi S, Takeuchi Y (1999) The cause of nontumorous defects of portal perfusion in the hepatic hilum revealed by CT during arterial portography. *AJR Am J Roentgenol* 172:397–402
 30. Couinaud C (1988) The parabiliary venous system. *Surg Radiol Anat* 10:311–316
 31. Chalasani N (2009) Nonalcoholic fatty liver disease liver fat score and fat equation to predict and quantitate hepatic steatosis: promising but not prime time! *Gastroenterology* 137:772–775